Imaging of Pulmonary Edema with Microwaves – Preliminary Investigation

Semih Doğu, İsmail Dilman, Mehmet Çayören and İbrahim Akduman

Electronics and Communication Engineering Dep.,
Istanbul Technical University, Istanbul, Turkey
dogu16@itu.edu.tr, dilman@itu.edu.tr, cayoren@itu.edu.tr, akduman@itu.edu.tr

Abstract

We consider microwave imaging of pulmonary edema which is a critical medical condition which manifests itself as a water accumulation in the human lungs. In order to detect water accumulation in the human lungs, we implement a microwave inversion scheme based on Born iterative method (BIM). To that end, a realistic human torso phantom is used and dielectric parameters of tissues and organs are estimated via Cole-Cole model at desired frequency. Then, scattered electric field is calculated synthetically by method of moments. Simulations are performed at 350 MHz and the region between phantom and antennas are surrounded by a dielectric material with a permittivity of 30. In the numerical results section, performance assessment of BIM is carried for two cases. The numerical results suggest that the BIM is capable of imaging water accumulation in the human lungs.

1. Introduction

According to World Health Organization (WHO), cardiovascular diseases (CVDs) are the most common cause of mortality and around the world over 17 million humans have died from CVDs in 2015. Increased blood pressure in the heart causes fluid accumulation in the air sacs of lungs and this pathological process is termed as pulmonary edema (PE). For this reason, monitoring of PE can be useful for early detection of hearth diseases.

In the literature, various methods have been proposed for detection of fluid accumulation in the air sacs of lung. Some of these methods provide information about presence of water without detecting its location, the other ones are capable of monitoring both the presence and the location of water accumulation. In [1], lungs are simply modeled with two sponges and presence of water is detected via utilization of changes of standing waves on the source. In another study, body area networking technologies are considered to estimate the average dielectric properties of lungs for detecting water accumulation [2]. Moreover, an audio signal based prototype is developed for determining fluctuation of water accumulation in a phantom [3].

All aforementioned studies are focused on determining the presence of water accumulation in the lungs. In recent years, two different approaches are commonly used for not only detecting the presence but also monitoring the location of water accumulation in lungs. In the earlier studies [4, 5], Electric Impedance Tomography (EIT) is preferred for acquiring images of the lungs. EIT systems are based on modeling of the tissues with lumped element approach. Afterwards, microwave imaging techniques have become quite popular with low operating costs, being harmless and being suitable for mobile applications

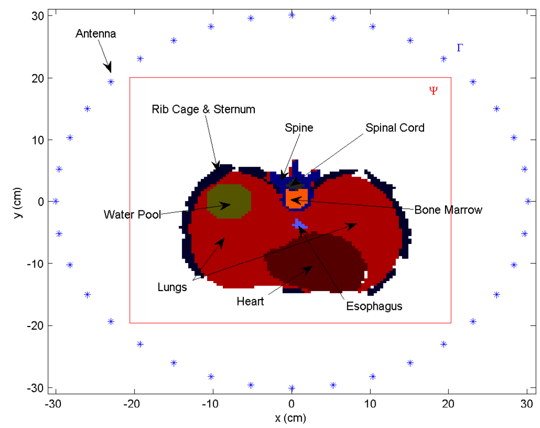

Figure 1. Simulation setup of human torso with the water accumulation. Antennas are depicted with asterisks. Ψ and Γ stand for investigated domain and circular measurement surface, respectively.

as compared to conventional medical imaging methods such as MRI, CT, PET and X-ray [6].

In this study, our aim is to demonstrate the capability to detect the water accumulation in the human lungs via Born Iterative Method (BIM), which is a well-established microwave imaging method. The BIM is applied in order to image water accumulation in a realistic human torso phantom. BIM is a fast converging iterative method and utilize the Born approximation. Through this procedure, the contrast function, which indicates the dielectric profile of tissues and organs, is reconstructed. Numerical simulations suggest that this microwave inversion method can be efficiently implemented in order to detect and to locate PE.

2. Formulation of the Problem

In order to monitor the pulmonary edema realistically in a human being, a 3-D human phantom composed of transmission computerized X-ray tomography images is used. A living adult male is used as a model for this phantom and the phantom can be reached in [7]. The phantom consists of $128\times128\times243$ images and a slice from upper part of torso is taken for performing simulations. The slice that we considered contains lungs, heart, esophagus, bone marrow, spinal cord, spine, rib cage, sternum, skin and skeletal muscles. In order to detect pulmonary edema, water accumulations are added inside the lungs. A mass of skin and skeletal muscles prevent electromagnetic waves to propa-

Table 1. 4-th order dielectric relaxation parameters of human tissues and organs in the torso.

Tissue	ϵ_∞	$\Delta\epsilon_1$	$\tau_1(ps)$	α_1	$\Delta\epsilon_2$	$\tau_2(ns)$	α_2	$\Delta\epsilon_3$	$\tau_3(\mu s)$	α_3	$\Delta\epsilon_4$	$\tau_4(ms)$	α_4	σ
Lung	2.5	18	7.96	0.1	500	63.66	0.1	2.5×10^5	159.15	0.2	4×10^7	7.958	0	0.03
Heart	4	50	7.96	0.1	1200	159.15	0.05	4.5×10^5	72.34	0.22	2.5×10^7	4.547	0	0.05
Esophagus	4	50	7.23	0.1	7000	353.68	0.1	1.2×10^6	318.31	0.1	2.5×10^7	2.274	0	0.2
B. Marrow	2.5	3	7.96	0.2	15	15.92	0.1	3.3×10^4	159.15	0.05	1×10^7	7.958	0.01	0.01
S. Cord	4	32	7.96	0.1	100	7.96	0.1	4×10^4	53.05	0.3	3.5×10^7	7.958	0.02	0.02
Spine	2.5	18	13.26	0.22	300	79.58	0.25	2×10^4	159.15	0.2	2×10^7	15.915	0	0.7
Sternum	2.5	10	13.26	0.2	180	79.58	0.2	5×10^3	159.15	0.2	21×10^5	15.915	0	0.02
Water	4.74	68.69	6.69	0	1.48	0.0015	0	0			0			0

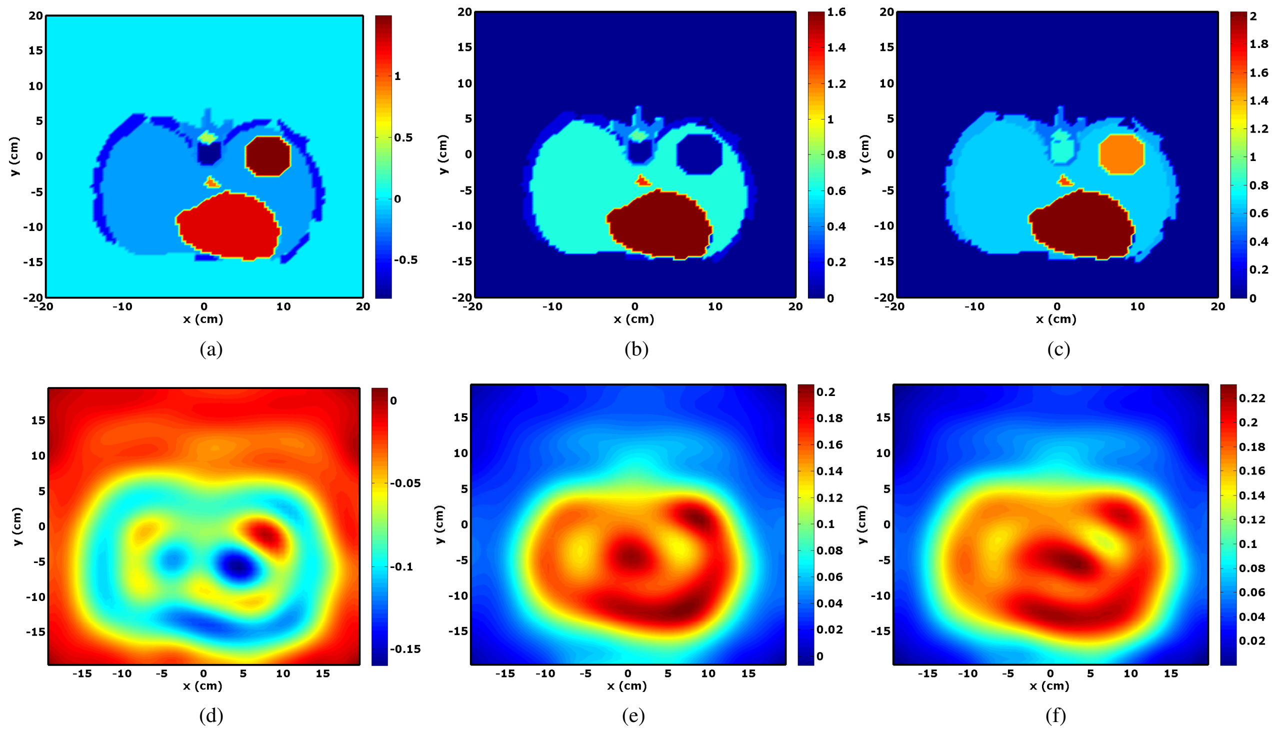

Figure 2. Pulmonary edema is occurred in the left lung. (a) Real value of actual contrast function, (b) imaginary value of actual contrast function and (c) absolute value of actual contrast function of human torso. (d) Real value of retrieved contrast function, (e) imaginary value of retrieved contrast function and (f) absolute value of retrieved contrast function via BIM at 350 MHz. The relative dielectric permittivity of matching medium between phantom and antennas is $\epsilon_b = 30$.

gate through the lungs therefore, for the sake of clarity, skin and skeletal muscles are extracted from phantom data. Location of antennas, phantom details and defined domains can be clearly seen in Fig.1. The time dependency of e^{-iwt} is assumed and omitted throughout the paper.

Multiple Cole-Cole model is used for determining dielectric properties of these biological tissues. This N-th order model reveals relative dielectric constant and conductivity of tissues and organs at the desired frequency as in [8],

$$\hat{\epsilon}(w) = \epsilon_\infty + \sum_{n=1}^{N} \frac{\Delta\epsilon_n}{1 + (-jw\tau_n)^{(1-\alpha_n)}} - \frac{\sigma}{jw\epsilon_0} \qquad (1)$$

where ϵ_∞, $\Delta\epsilon_n$, τ_n, α_n, σ and ϵ_0 stand for permittivity at infinite frequency, magnitude of dispersion, relaxation time constant, distribution parameter, static conductivity and permittivity of free space, respectively. Angular frequency is denoted by w. The parameters of biological tissues and organs are taken from [8] and parameters of water are taken from [9]. These parameters are represented in Table 1 for 4-th order Cole-Cole model. Then, method of moment is implemented in order to calculate scattered field from phantom by using the technique proposed in [10]. Transverse magnetic (TM) line sources are used for excitation.

3. Quantitative Microwave Inversion Method

The aim of quantitative microwave inversion methods is to detect objects in the investigated domain by retrieving contrast function χ. Born Iterative Method (BIM) is one of these meth-

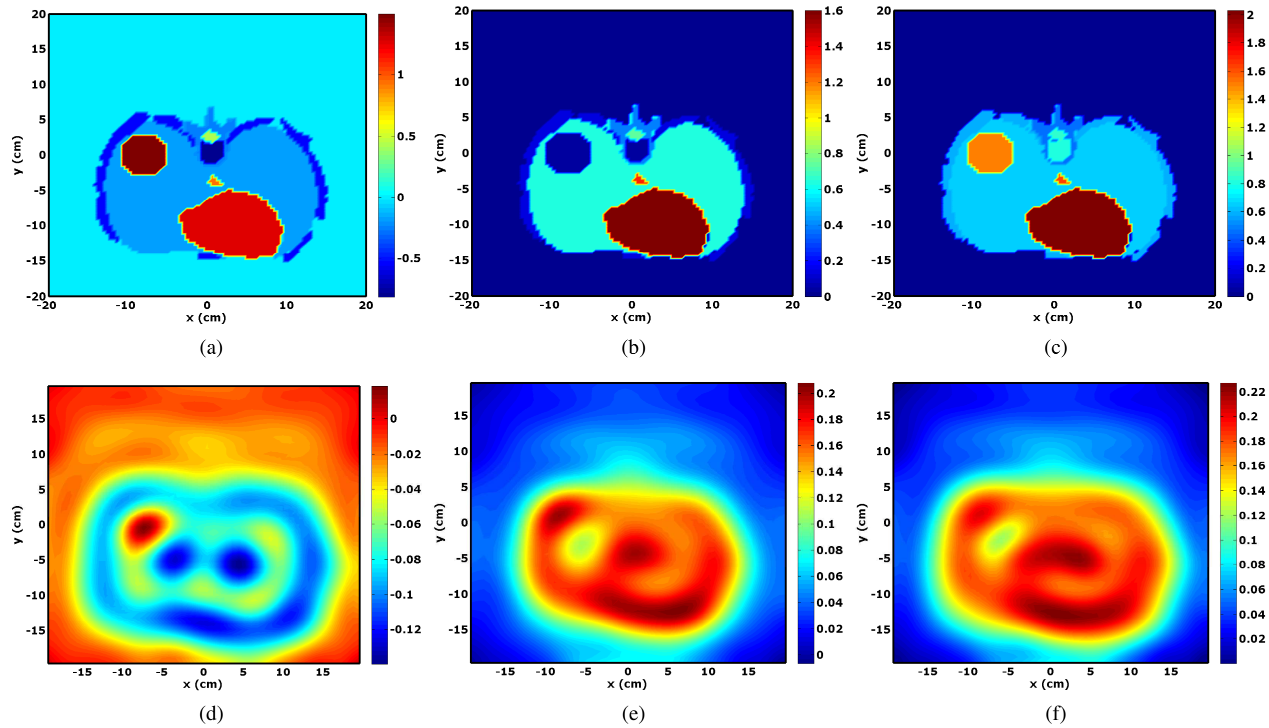

Figure 3. Pulmonary edema is occurred in the right lung. (a) Real value of actual contrast function, (b) imaginary value of actual contrast function and (c) absolute value of actual contrast function of human torso. (d) Real value of retrieved contrast function, (e) imaginary value of retrieved contrast function and (f) absolute value of retrieved contrast function via BIM at 350 MHz. The relative dielectric permittivity of matching medium between phantom and antennas is $\epsilon_b = 30$.

ods and estimates contrast function by solving an integral based system. The well established iterative scheme of BIM is first presented in [11] for the 2-D TM case. For the sake of simplicity, TM incident line sources are considered in this study.

BIM determines contrast function of scatterers by measuring scattered field in the observation domain Γ and by calculating incident field in the investigated domain Ψ in a way similar to the other microwave inversion methods. The symbolical representation of scattered field U^s can be formulated as,

$$U^s = G_\Gamma \chi U^t \tag{2}$$

and (2) is called as the data equation in microwave inverse theory. Another significant equation which is called as the object equation based on calculating total field U^t is given as,

$$U^t = U^i + G_\Psi \chi U^t \tag{3}$$

Here G_Ψ and G_Γ are integral operators with respect to domain Ψ and Γ, U^i stands for incident field. These integral operators are defined as,

$$G_{\Psi,\Gamma}\chi(\rho')U^t(\rho') = \int_{\Psi,\Gamma} g(\rho,\rho')\chi(\rho')U^t(\rho')dv(\rho') \tag{4}$$

where ρ and ρ' denote source point and observation point, respectively and g stands for 2-D scalar Green's function. Basically, BIM aims to solve following minimizing function to reconstruct electrical profile of objects,

$$\chi_{n+1} = argmin \frac{\sum_{j=1}^{J} \|U_j^s - G_\Gamma \chi_n U_{j,n}^t\|_\Gamma^2}{\sum_{j=1}^{J} \|U_j^s\|_\Gamma^2} \tag{5}$$

where $\|\cdot\|_\Gamma$ indicates L_2 norm on domain Γ, J and n stand for total number of transmitting antennas and iteration count, respectively. Initial guess may be chosen $\chi_0 = 0$ for the contrast function but other predictions are also acceptable. In this study, initial value of contrast function is calculated by solving (5) under Born approximation. Born approximation states that if the object is a weak scatterer, scattered field becomes much smaller than the incident field on the object, therefore, total field may be assumed to be equal to the incident field on the object.

4. Numerical Results

In order to assess the performance of BIM algorithm to detect pulmonary edema, two simulation examples are carried out. First, the case of water accumulation occurred in the left lung is considered. Afterwards, the position of water accumulation is shifted to right lung. The operating frequency is selected as 350 MHz which is acceptable in medical microwave applications for getting accurate results. Likewise, we consider that the medium between antennas and phantom is filled a non conductive dielectric material. The main advantages of using matching medium with relative dielectric constant of 30 is letting electromagnetic waves propagate into the inner parts of the lungs. Otherwise, the effects of inner parts on the scattered field can not be observed.

The water accumulation with circular shape has a radius of 3 cm and it is centered at $x = 8$ cm and $y = 0$ cm for the first measurement. The real, imaginary and absolute values of the complex dielectric permittivity of all tissues and organs in the phantom are shown in Fig 2(a)-(c), respectively. The water has the highest real dielectric permittivity value and the lowest complex dielectric permittivity value with respect to other tissues and organs. The reconstruction of the real part for the first simulation is demonstrated in Fig. 2(d) and it can be commented that the water region can be seen in phantom area. It can be also said that the presence of high dielectric and conductive tissues and organs masks the contribution of the water to the contrast function χ. Imaginary and absolute values of reconstructed χ are depicted in Fig 2(e)-(f), respectively. In the second simulation, the center of water accumulation shifts to $x = -8$ cm and $y = 0$ cm. Actual and reconstructed results are represented in Fig. 3 for second simulation setup. After the position change of the water accumulation, same results are obtained and the comments for the first simulation setup can be reiterated.

5. Conclusion

In this study, a microwave inversion technique named Born iterative method is applied in order to monitor water accumulation in the human lungs. For this purpose, a realistic human torso phantom is considered and the scattered electric field calculated synthetically via method of moments. Electrical properties of tissues and organs are calculated using Cole-Cole model at desired frequency. Two scenarios with edema at different positions are carried out in order to test the inversion algorithm. The reconstructed results are partly promising while proper matching medium is chosen. This study can be extended to 3-D realistic human phantom and finally experimental data can be implemented to inversion algorithms.

6. Acknowledgment

This work is supported by The Scientific and Technological Research Council of Turkey (TUBITAK) under the project 216S415.

7. References

[1] C. Susskind, “Possible use of microwaves in the management of lung disease,” *Proceedings of the IEEE*, vol. 61, no. 5, pp. 673–674, 1973.

[2] S. Salman, Z. Wang, E. Colebeck, A. Kiourti, E. Topsakal, and J. L. Volakis, “Pulmonary edema monitoring sensor with integrated body-area network for remote medical sensing,” *IEEE transactions on Antennas and Propagation*, vol. 62, no. 5, pp. 2787–2794, 2014.

[3] K. Mulligan, A. Adler, and R. Goubran, “Detecting regional lung properties using audio transfer functions of the respiratory system,” in *Engineering in Medicine and Biology Society, 2009. EMBC 2009. Annual International Conference of the IEEE*. IEEE, 2009, pp. 5697–5700.

[4] J. C. Newell, P. Edic, X. Ren, J. Larson-Wiseman, and M. Danyleiko, “Assessment of acute pulmonary edema in dogs by electrical impedance imaging,” *IEEE Transactions on Biomedical Engineering*, vol. 43, no. 2, pp. 133–138, 1996.

[5] E. J. Woo, P. Hua, J. G. Webster, and W. J. Tompkins, “Measuring lung resistivity using electrical impedance tomography,” *IEEE transactions on biomedical engineering*, vol. 39, no. 7, pp. 756–760, 1992.

[6] S. Semenov, “Microwave tomography: review of the progress towards clinical applications,” *Philosophical Transactions of the Royal Society of London A: Mathematical, Physical and Engineering Sciences*, vol. 367, no. 1900, pp. 3021–3042, 2009.

[7] I. G. Zubal, C. R. Harrell, E. O. Smith, Z. Rattner, G. Gindi, and P. B. Hoffer, “Computerized three-dimensional segmented human anatomy,” *Medical Physics*, vol. 21, no. 2, pp. 299–302, 1994.

[8] S. Gabriel, R. W. Lau, and C. Gabriel, “The dielectric properties of biological tissues: Iii parametric models for the dielectric spectrum of tissues,” *Physics in Medicine & Biology*, vol. 41, no. 11, p. 2271, 1996.

[9] R. Buchner, J. Barthel, and J. Stauber, “The dielectric relaxation of water between $0^{\circ}c$ and $35^{\circ}c$,” *Chemical Physics Letters*, vol. 306, no. 1, pp. 57 – 63, 1999.

[10] J. Richmond, “Scattering by a dielectric cylinder of arbitrary cross section shape,” *IEEE Transactions on Antennas and Propagation*, vol. 13, no. 3, pp. 334–341, May 1965.

[11] Y. M. Wang and W. C. Chew, “An iterative solution of the two-dimensional electromagnetic inverse scattering problem,” *International Journal of Imaging Systems and Technology*, vol. 1, no. 1, pp. 100–108, 1989.